

Article

Biodiesel Production via Transesterification Reaction over Mono- and Bimetallic Copper-Noble Metal (Pt, Ru) Catalysts Supported on BEA Zeolite

Łukasz Szkudlarek , Karolina Chałupka-Śpiwak , Waldemar Maniukiewicz , Jadwiga Albińska, Małgorzata Iwona Szykowska-Jóźwik  and Paweł Mierczyński * 

Institute of General and Ecological Chemistry, Lodz University of Technology, Zeromskiego 116, 90-924 Lodz, Poland; lukasz.szkudlarek@dokt.p.lodz.pl (Ł.S.); karolina.chalupka@p.lodz.pl (K.C.-Ś.); waldemar.maniukiewicz@p.lodz.pl (W.M.); jadwiga.albinska@p.lodz.pl (J.A.); malgorzata.szykowska@p.lodz.pl (M.I.S.-J.)

* Correspondence: pawel.mierczynski@p.lodz.pl; Tel.: +48-42-631-31-25; Fax: +48-42-631-31-28

Abstract: This work focuses on the study of biodiesel production from commercial rapeseed oil and methanol via transesterification reactions on monometallic copper and bimetallic copper-noble metal (platinum, ruthenium) catalysts supported on BEA zeolite. The catalysts were prepared by wet impregnation method on the hydrogen form of BEA zeolite. As part of the study, the physicochemical and catalytic properties of the prepared catalytic materials were determined. The catalytic activity tests were carried out in the transesterification reaction over prepared catalysts at 220 °C for 2 h in an autoclave. The physicochemical properties of the obtained catalysts were investigated by X-ray diffraction (XRD), specific surface area and porosity (BET), a scanning electron microscope equipped with an energy dispersive spectrometer (SEM-EDS) and temperature-programmed desorption of ammonia (TPD-NH₃) method. The results of the catalytic activity showed the promotional effect of the noble metal on the TG conversion and FAME efficiency of copper catalysts in the biodiesel production process. The most active catalyst turned out to be the calcined 5%Cu-1%Ru/BEA catalyst, which showed the highest TG conversion of 85.7% and the second highest FAME efficiency of 58.4%. The high activity of this system is explained by its surface acidity and large specific surface area.

Keywords: BEA; transesterification reaction; zeolite catalysts; biodiesel production; copper catalysts; noble metal



Citation: Szkudlarek, Ł.; Chałupka-Śpiwak, K.; Maniukiewicz, W.; Albińska, J.; Szykowska-Jóźwik, M.I.; Mierczyński, P. Biodiesel Production via Transesterification Reaction over Mono- and Bimetallic Copper-Noble Metal (Pt, Ru) Catalysts Supported on BEA Zeolite. *Catalysts* **2024**, *14*, 260. <https://doi.org/10.3390/catal14040260>

Academic Editor: Narendra Kumar

Received: 24 March 2024

Revised: 7 April 2024

Accepted: 10 April 2024

Published: 14 April 2024



Copyright: © 2024 by the authors. Licensee MDPI, Basel, Switzerland. This article is an open access article distributed under the terms and conditions of the Creative Commons Attribution (CC BY) license (<https://creativecommons.org/licenses/by/4.0/>).

1. Introduction

The main driving force in socio-economic development, which includes transportation, technological advancement and industrialization, is energy [1]. The global energy demand has increased significantly due to rapid industrialization, modernization and increasing population [2]. The availability of fossil-fuel-derived energy at the levels required by industrial societies is a problem at social, political and commercial levels [3]. The main advantage of biodiesel is that it can be used in compression ignition engines without modification. Biodiesel can completely or partially replace conventional diesel fuel [4]. Biodiesel has a number of advantageous physicochemical properties, including a high flash point, high lubricity, high biodegradability [5] and better viscosity with similar caloric performance to conventional fossil fuels [6]. The combustion of biodiesel is better due to the oxygen content in the composition of FAME. Furthermore, biodiesel can be blended in any proportion with conventional petroleum-based diesel [7]. Biodiesel is considered an environmentally friendly, clean, renewable and sustainable fuel [8–14]. The combustion of biodiesel produces lower emissions of gaseous pollutants (i.e., SO_x, NO_x, CO and HC) as well as particulate matter or soot compared to conventional diesel fuel [15]. Biodiesel is synthesized via the transesterification reaction of triglycerides derived from vegetable oils with

a short-chain alcohol. The reaction can be catalyzed by homogeneous or heterogeneous catalysts [16]. The main disadvantages of homogeneous catalysts include the difficulty or impossibility of their reuse and susceptibility to deactivation in the presence of water and free fatty acids in the starting raw material [17]. To avoid problems associated with the use of homogeneous catalysts in the transesterification of triglycerides, a viable solution is to replace them with heterogeneous catalysts [18]. Compared to homogeneous catalysts, the use of a heterogeneous catalyst in the transesterification reaction has great advantages, because it can be more easily separated from the products and the biodiesel can be purified more easily after the reaction [19]. In addition, an important feature of heterogeneous catalysts is the possibility of their regeneration [14]. The most commonly used heterogeneous catalysts are alkali metal oxides (e.g., CaO, MgO and BaO) and transition metal oxides (e.g., ZrO₂, MnO, ZnO and MoO), which are used directly or in a modified form [20]. Zeolites play a fundamental role as reaction catalysts in the conversion of biologically derived molecules into biofuels, chemicals and other materials [21]. Zeolites are crystalline aluminosilicates that are characterized by a microporous structure. The stable crystal structure of zeolites consists of a combination of silicate and aluminate tetrahedra. However, this combination leads to a charge imbalance, causing zeolites to have acidic properties [22]. The acid-base properties of zeolites are determined by the ratio of silicon to aluminum. In addition to the acid-base properties, the catalytic properties of zeolites and catalyst systems based on these materials depend on the form, shape or amount of the active component [23].

To date, there is no mention in the literature data of the use of copper-based catalyst systems on zeolites, applied in biodiesel production via the transesterification reaction of triglycerides from rapeseed oils or algae. Copper-zeolite catalysts are widely used in, e.g., selective catalytic reduction (SCR) [24,25], selective hydrodeoxygenation [26], selective catalytic oxidation [27], propane oxidation [28], bio-oil deoxygenation [29], and oxidation of methane to methanol [30–32]. In the previous work [11], noble metals (Ag, Pd, Pt, and Ru) supported on natural zeolite were examined in the transesterification reaction of rapeseed oil with methanol towards biodiesel production. The introduction of a noble metal onto the surface of natural zeolite has been shown to improve the yield of methyl esters obtained and the TG conversion of the natural zeolite. Despite the high triglyceride conversion and biodiesel yield, the transesterification reaction was conducted at an elevated temperature (260 °C). Moreover, the metals used in the study are very expensive due to their limited availability. As a cheaper metal, copper can be an alternative to precious metals. Furthermore, addition of a small amount of precious metal to copper catalyst can lower the process temperature and improve the stability of copper catalysts in the production of biodiesel.

The aim of this work was to determine the catalytic activity of copper and bimetallic copper-noble metal (Pt, Ru) catalysts supported on BEA zeolite, in the transesterification reaction of rapeseed oil with methanol. In addition, the effect of a noble metal addition to the Cu/BEA catalyst on its physicochemical and catalytic properties was also investigated. The physicochemical properties of the synthesized catalysts were studied using the following research techniques: TPR-H₂, BET, XRD, TPD-NH₃ and SEM-EDS. The results of the physicochemical properties studies were correlated with the catalytic activity of the synthesized catalysts used in the transesterification reaction.

2. Results

2.1. Catalytic Activity

The catalytic activity studies of copper-based zeolite catalysts were carried out in the transesterification reaction of rapeseed oil with methanol at a temperature of 220 °C for 2 h using an autoclave with continuous stirring of the reagents. The catalysts evaluated in the process were previously calcined at 500 °C for 4 h in an air atmosphere or calcined under the same conditions and reduced for 2 h at 300 °C or 400 °C in a reducing mixture (5% H₂–95% Ar) and then tested in the biodiesel production process. The activity of the investigated catalytic systems was expressed as the values of triglycerides (TGs) conversion

and the yield of fatty acid methyl esters (FAME). The results of the catalytic tests performed in the studied reaction are shown in Figure 1, Figure 2 and Table 1. The catalytic activity of the calcined and reduced mono-(5 wt% Cu and 10 wt% Cu) and bimetallic (Pt-Cu, Ru-Cu) catalysts showed a high triglyceride conversion in the range of 73.6–85.1%. It was found that such high TG conversions were observed independently of copper content and the oxidation state of the active phase components. However, significant differences in biodiesel efficiency were observed between the calcined and reduced systems. Both the 5% Cu/BEA and 10% Cu/BEA calcined systems showed approximately 10% higher FAME efficiency than the reduced catalysts. The reactivity results obtained for both the calcined and reduced catalysts showed that the introduction of a noble metal (1 wt.%) to the copper catalyst supported on the zeolite improved TG conversion in the investigated process by 7 to 10%. Furthermore, the FAME yields calculated for the studied catalysts showed that the introduction of noble metal into the calcined Cu catalyst also led to higher FAME yields, increasing by about 4% for the reaction performed on the calcined 5%Cu–1%Pt/BEA system, and by around 7% for the transesterification process realized on the calcined 5%Cu–1%Ru/BEA catalyst. In the case of the reduced catalysts, an improvement in FAME yields for bimetallic catalysts compared to the reduced monometallic catalyst was also observed. FAME yield increased approximately by about 1.9% for the reaction performed on the 5%Cu–1%Pt/BEA catalyst and by approx. 3% for the transesterification realized on the reduced 5%Cu–1%Ru/BEA catalyst. The lowest TG conversion (56.3%) and FAME yield (28.2%) were detected in the transesterification process carried out over unmodified zeolite BEA. Among all the catalytic materials containing 5 wt. % of Cu tested in the transesterification reaction, the highest TG conversion (85.1%) and the highest FAME yield (58.4%) were confirmed for the calcined 5%Cu–1%Ru/BEA system. On the other hand, among all the reduced catalysts containing 5 wt. % of Cu investigated in the biodiesel production process, the highest FAME yield equal to 45.5% was recorded for the 5%Cu–1%Ru/BEA catalyst, but the highest TG conversion equal to 82.4% was confirmed for the reduced 5%Cu–1%Pt/BEA system. Based on the obtained results for catalytic activity in the transesterification reaction, it is possible to observe the influence of the reduction process and the promotion of the copper catalyst by a noble metal on the values obtained for triglyceride conversion and the yield of methyl esters of higher fatty acids. In the case of bimetallic catalysts, the obtained results confirmed an increase in the conversion of triglycerides and the yield of the obtained methyl esters compared to the monometallic catalysts. The reduction process of the 5%Cu–1%Pt bimetallic catalyst did not lead to a change in the value of the triglyceride conversion but it resulted in a decrease in the yield of esters produced in the investigated reaction, compared to the same catalyst after calcination. However, in the case of the 5%Cu–1%Ru catalyst, its reduction led to a lower TG conversion value and FAME efficiency compared to the same catalyst after calcination. If we compare the catalytic activity results obtained for the bimetallic catalysts after reduction with the monometallic catalysts after both calcination and reduction, their higher conversion of triglycerides in the studied process was confirmed. However, regarding the yield of methyl esters for the bimetallic catalysts after reduction, the activity measurements showed lower efficiency values compared to the catalysts after calcination, but higher values than the 5%Cu/BEA catalyst after the reduction process.

In the case of copper catalysts with a higher copper content in the system (10 wt.% of Cu), the catalytic activity tests conducted in the tested reaction confirmed higher triglyceride conversion values and higher yields of methyl esters compared to their analogues containing 5 wt.% of copper. Chang et al. [33] investigated a copper-based supramolecular catalyst on β -cyclodextrins (β -CD) in the transesterification reaction of Xanthium sibiricum Patr oil. The Cu– β -CD catalyst was evaluated in a reaction carried out in a glass three-necked flask with a condensing means placed in an oil bath. The transesterification reaction was performed at 120 °C for 9 h with a methanol to oil ratio of 40:1, using 8% by weight of the catalyst. The obtained results showed that the Cu– β -CD catalyst showed high activity under these reaction conditions, producing biodiesel with a FAME efficiency of 88.63%.

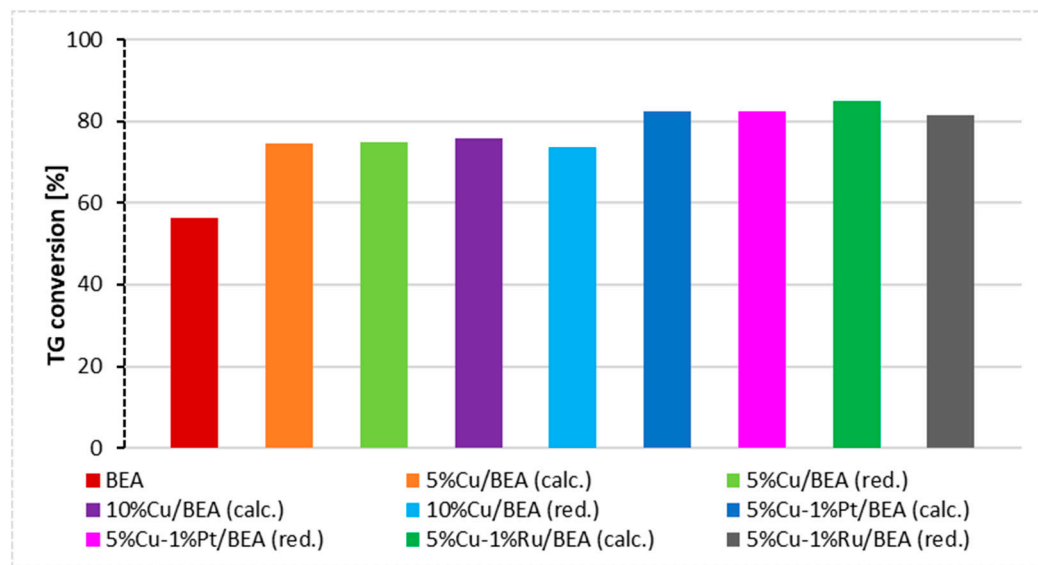


Figure 1. TG conversions of mono- and bimetallic (copper–noble metal (Pt, Ru)) catalysts supported on BEA zeolite in transesterification reaction.

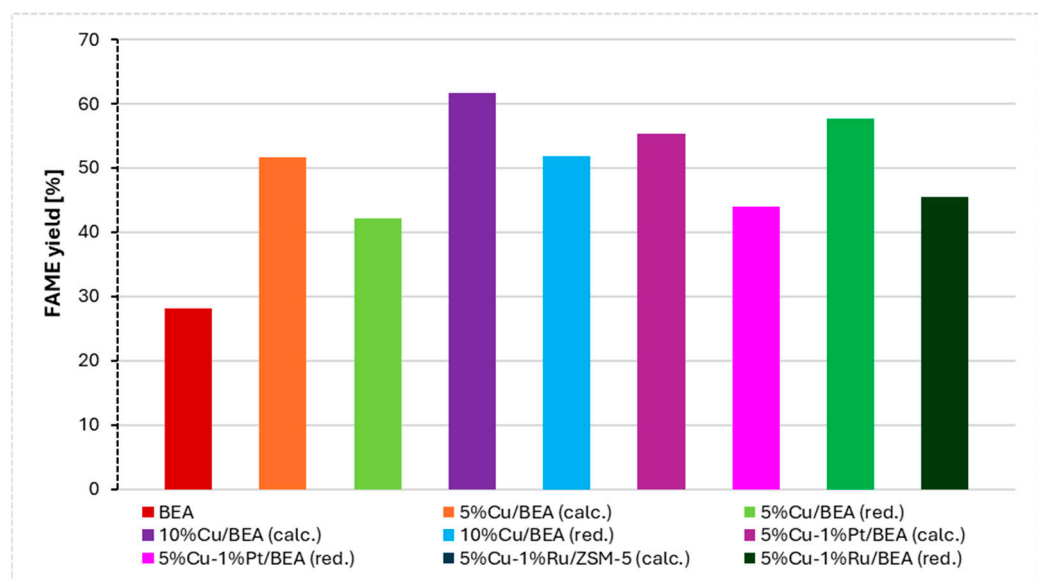


Figure 2. FAME yields of mono- and bimetallic (copper–noble metal (Pt, Ru)) catalysts supported on BEA zeolite in transesterification reaction.

Table 1. The catalytic activity results obtained in the transesterification reaction over BEA, mono- and bimetallic catalysts calcined or calcined and reduced in a mixture of 5% H_2 –95%Ar at 300 or 400 °C for 2 h.

Catalyst	Triglycerides Conversion [%]	FAME Yield [%]
BEA	56.3	28.2
5%Cu/BEA (calc.)	74.5	51.7
5%Cu/BEA (red.)	74.8	42.1
10%Cu/BEA (calc.)	75.7	61.6
10%Cu/BEA (red.)	73.6	51.9
5%Cu–1%Pt/BEA (calc.)	82.5	55.4
5%Cu–1%Pt/BEA (red.)	82.4	44.0
5%Cu–1%Ru/BEA (calc.)	85.1	58.4
5%Cu–1%Ru/BEA (red.)	81.5	45.5

Pangestu and co-workers [34] investigated a heterogeneous copper-based catalytic system in a metal–organic framework (MOF), which was synthesized from the coordination of benzene-1,3,5-tricarboxylic acid (BTC) and divalent copper. The transesterification reaction was conducted in a three-neck flask at 60 °C for 4 h. The reaction mixture contained 5 g of palm oil with 0.04 g of metal–organic framework in 50 mL of methanol. The authors revealed that the optimum FAME yield (91.0%) was reached in the transesterification reaction with 0.04 g CuBTC and the volume of MeOH:oil equal to 5:1. Moreover, after regeneration, this catalytic material was able to produce biodiesel with a yield of 86.0% FAME in the tested reaction. The authors also observed that CuBTC–MOF has high thermal stability. Silva et al. [35] tested catalysts in the form of Cu(II) and Co(II) ions adsorbed in chitosan, used in the transesterification of soybean and babassu oils. The catalytic activity tests were performed in a 250 mL two-necked flask fitted with a water-cooled condenser at 70 °C for 3 h in pH 8.5. The reaction mixture contained 100 g of oil (soybean or babassu), 20 g of methanol and 2 g of catalyst. The authors reported that copper-based catalysts exhibited high biodiesel yields of 88.82% (for soybean oil) and 71.89% (for babassu oil). Chen and co-authors [36] conducted another study concerning biodiesel production over copper-based catalysts. They studied biodiesel production over copper vanadium phosphate catalyst (CuVOP) in the transesterification of soybean oil. The reaction was carried out in a flask equipped with a magnetic stirrer, a reflux condenser and a thermometer. The process was carried out in the temperature range of 40–80 °C for 3–7 h, using a molar ratio of methanol to oil of 4:1–8:1 and using from 1% to 5% by weight of the catalyst. It was found that the highest conversion was exhibited during the process performed at 65 °C for 5 h with a molar ratio of methanol/oil equal 6.75 containing 1.5% of CuVOP system.

2.2. Specific Surface Area Measurements

Specific surface area (SSA) measurements taken for monometallic copper catalysts and bimetallic Cu–noble metal (Pt, Ru) catalysts are presented in Table 2. The results show that the largest specific surface area (490 m²/g) was measured for the 5%Cu/BEA reduced at 300 °C for 2 h in a mixture of 5%H₂–95%Ar. After calcination, the same catalyst had a lower SSA value of 467 m²/g. Increasing the copper content in the monometallic catalyst to 10% by weight led to a decrease in the SSA value by approximately 47 m²/g for the reduced system and by approximately 60 m²/g for the calcined system. After calcination, the 10%Cu/BEA catalyst was characterized by the lowest SSA value (407 m²/g) among all the tested catalysts. It is also worth noting that the calcined 10%Cu/BEA catalyst showed the smallest external surface area, the smallest micropore area measured with the t-plot method, and the smallest pore and micropore volumes. The average pore size for this catalyst was lower than for the same catalyst after reduction. In addition, monometallic 10%Cu/BEA catalyst after reduction was characterized by the second lowest specific surface area (443 m²/g), a micropore surface area equal to 280 m²/g, an external surface area value of 163 m²/g and the average pore size of 8.01 nm. Additionally, in the case of catalysts containing 10 wt.% of Cu, a decrease in the pore volume and micropore volume was observed compared to the 5%Cu/BEA catalysts. The introduction of 1% platinum onto the surface of the 5%Cu/BEA catalyst after calcination did not change the SSA surface area for the calcined 5%Cu–1%Pt/BEA system, while after reduction, this catalyst specific surface area decreased by 8 m²/g compared to its monometallic counterpart. The volume of pores and micropores for this bimetallic catalyst after calcination was 0.689 and 0.154, respectively. These values were lower than for the monometallic catalysts. However, in the case of the 5%Cu–1%Pt/BEA catalyst after reduction, the pore and micropore volume values were higher than the calcined copper catalyst and were equal to 0.747 and 0.159, respectively. This catalyst also showed a higher average pore size value of 7.96 nm compared to the reduced monometallic catalyst. In the case of the 5%Cu–1%Ru/BEA catalyst after calcination and after reduction, the specific surface area and microporous surface were lower than for the corresponding copper monometallic catalysts. The size of the external surface measured for the 5%Cu–1%Ru/BEA bimetallic catalyst after calcination and reduction was higher

than both the monometallic catalysts and the corresponding bimetallic catalysts containing 1% by weight of Pt. It is worth noting that the 5%Cu–1%Ru/BEA bimetallic catalysts after calcination and reduction were characterized by the highest external surface area value, and the difference in the average pore size of both catalysts was not significant. The measurements showed that in the case of reduced catalysts, in addition to the increase in the external surface and the surface of the micropores, the volume of pores and micropores also increased with the average pore size compared to the calcined catalysts. The only exception is the reduced 5%Cu/BEA system, for which the average pore size was smaller.

Table 2. Specific surface area, micropore area, external surface area, pore volume, micropore volume and pore size distributions of mono- and bimetallic catalysts supported on BEA zeolite calcined in an air atmosphere at 500 °C for 4 h.

Catalyst	BET Surface Area (m ² /g)	t-Plot Micropore Area (m ² /g)	t-Plot External Surface Area (m ² /g)	Pore Volume (cm ³ /g)	t-Plot Micropore Volume (cm ³ /g)	Average Pore Size (nm)
5%Cu/BEA (calc.)	467	299	168	0.706	0.155	7.80
5%Cu/BEA (red.)	490	311	179	0.719	0.161	7.44
10%Cu/BEA (calc.)	407	252	155	0.663	0.131	7.88
10%Cu/BEA (red.)	443	280	163	0.703	0.145	8.01
5%Cu–1%Pt/BEA (calc.)	467	297	170	0.689	0.154	7.59
5%Cu–1%Pt/BEA (red.)	482	307	174	0.747	0.159	7.96
5%Cu–1%Ru/BEA (calc.)	454	274	180	0.729	0.141	7.41
5%Cu–1%Ru/BEA (red.)	482	300	181	0.739	0.155	7.45

2.3. Reducibility of Mono- and Bimetallic Cu Catalysts

In this paper, the reduction behaviour of the obtained copper catalytic systems supported on zeolite was investigated using the temperature-programmed reduction (H₂-TPR) technique. The H₂-TPR results of the studied systems are presented in Figure 3. TPR profiles recorded for the 5%Cu/BEA and 10%Cu/BEA catalysts showed one reduction peak. The maxima of the reduction peaks recorded for these catalysts were visible at around 230 °C. The single reduction peaks recorded for monometallic catalysts are assigned to the reduction of CuO to metallic copper. It is well known in the literature data that a copper supported catalyst might be reduced in one or two reduction stages [37,38]. The literature data concerning of a two-stage reduction mechanism of copper catalysts assumes the reduction of CuO to metallic copper through Cu₂O species. Schaidle et al. [39] synthesized a Cu/BEA catalyst for the conversion of dimethyl ether to 2,2,3-trimethylbutane and studied its reducibility. In their research, the H₂-TPR profile of a copper–zeolite catalyst also showed only one reduction peak, situated at 255 °C and assigned to the reduction of CuO to metallic copper. According to Lin and co-authors [40], the one-step reduction of the active phase of the copper-based catalyst indicates that after the calcination of the catalyst system, the active phase occurs in the form of aggregated CuO. Research data from the literature also shows that copper catalysts are reduced through a two-stage reduction mechanism. This is particularly true for isolated copper ions (Cu²⁺) that occur in the pores of the BEA zeolite. Wang et al. [41], investigated zeolite structure effects on Cu active center, SCR performance and the stability of Cu–zeolite catalysts. Authors in their work studied the reducibility of a copper catalyst supported on various zeolite supports such as Beta, ZSM-5, Y, Offretite, ZSM-34, UZM-12, SSZ-13, SSZ-16 and SSZ-17. The authors observed an intensive reduction peak for the Cu–Beta sample below 300 °C. This intensive reduction peak, which was visible on the TPR profile, was split into three reduction peaks. The first peak starting at 200 °C is attributed to the reduction of isolated Cu²⁺ to Cu⁺. The next reduction peak with a maximum hydrogen consumption at around 250 °C is attributed to the reduction of CuO particles to metallic copper (Cu⁰). The last peak, which ends at a temperature of approximately 300 °C, is associated with the reduction of Cu⁺ to

metallic Cu^0 . In this work also reduction behaviour of bimetallic catalysts supported on BEA zeolite was studied. In the case of the bimetallic catalysts, more than one reduction stage was observed in the TPR profiles recorded for these catalysts. In the temperature-programmed reduction profile of the bimetallic 5%Cu–1%Ru/BEA, three unresolved peaks were observed on the TPR- H_2 profile. The first two reduction effects were visible in the temperature range 130–180 °C. Those reduction effects are assigned to the reduction of RuO_2 species through RuO to metallic Ru. The next reduction effect situated in the temperature range 190–310 °C is assigned to the reduction of CuO to metallic Cu [42,43]. In our previous work [44], we also studied the reduction behaviour of Ru-supported catalysts and we observed also two reduction stages on the TPR curve, which were assigned to the reduction of RuO_2 to metallic Ru through RuO species. The same reduction mechanism of a Ru catalyst was confirmed by Nurunnabi et al. [45]. As for the ruthenium-containing zeolite catalyst, Serrano and co-workers [46] studied the hydroreforming of LDPE thermal cracking oils using an Ru1%/h-Beta catalyst (hierarchical zeolite). On the H_2 -TPR profile, the researchers observed one reduction peak with a maximum occurring at 156 °C, which refers to a one-step total reduction of RuO_2 . The reduction of RuO_2 particles in the temperature range of 155–157 °C has also been confirmed by Glotov and co-workers [47] in studies of ruthenium catalysts templated on MCM-41-type mesoporous silica and natural clay nanotubes. The reduction measurement recorded for a bimetallic 5%Cu–1%Pt/BEA catalyst showed that this system is reduced in two stages. Those two stages are connected with the reduction of PtO_2 and CuO species, respectively. The first reduction stage situated in the temperature range 150–220 °C is assigned to the reduction of PtO_2 . While the second reduction stage located in the temperature range 215–275 °C may be connected with the reduction of CuO species to metallic copper and with the two steps mechanism of CuO reduction to metallic copper through Cu_2O species. The work published by Pérez-Bustos et al. [48] confirms the reduction of Pt^{4+} and Pt^{2+} species to Pt^0 occurring at temperatures ranging from 180 °C to 230 °C. In addition, the reduction peak assigned to PtO can be visible on the TPR profile in the temperature range 170–270 °C [49].

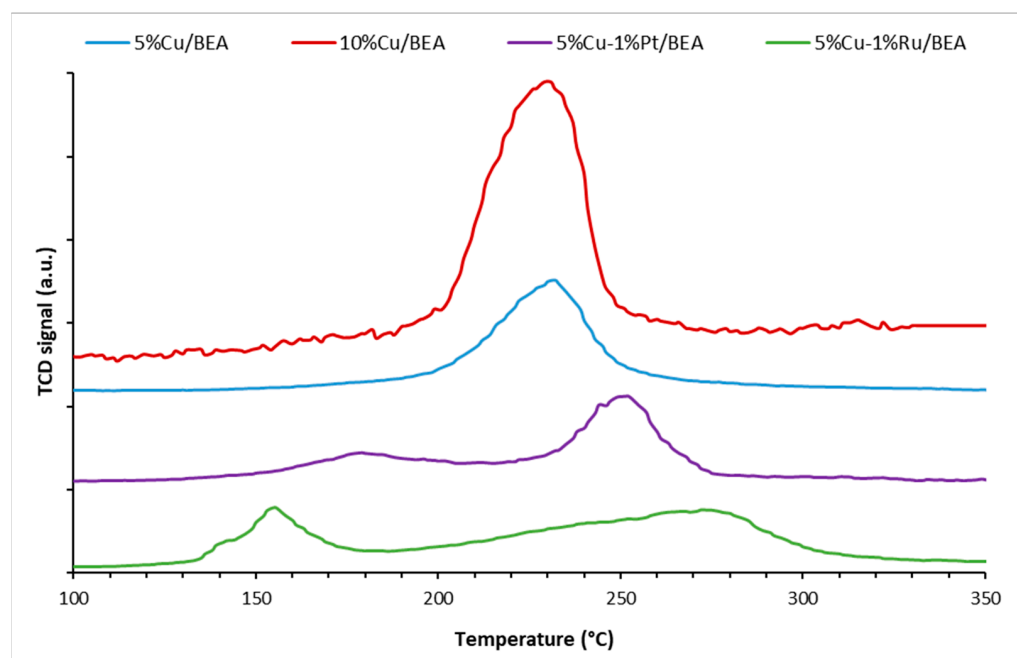


Figure 3. H_2 -TPR curves recorded for Cu/BEA and Cu–M (M = Ru, Pt) zeolite catalysts calcined in an air atmosphere for 4 h at 500 °C.

2.4. The Acidity of the Investigated Catalysts

A temperature-programmed desorption method using ammonia as a probe molecule was used to determine the acidic properties of the studied catalytic material. The results are shown in Table 3. The acid centers were determined and divided into weak-strength acid centers (in the temperature range of 100–300 °C), moderate-strength acid centers (300–450 °C) and strong-strength acid centers (>450 °C) for all the examined samples. The surface acidity was calculated based on the area under the desorption peak and the results were expressed as total acidity per gram of the catalytic material. The desorption of ammonia was performed in the temperature range of 100 to 600 °C. The total acidity of the investigated calcined catalysts Cu or Cu–M (M = Ru, Pt) is arranged in descending order: 10%Cu/BEA > 5%Cu–1%Ru/BEA > 5%Cu/BEA > 5%Cu–1%Pt/BEA. An increase in copper content from 5 wt.% up to 10% by weight resulted in a significant increase in high-strength acid centers and an increase in moderate-strength acid centers. The addition of ruthenium to the calcined system contributed to a slight increase in total acidity by increasing the number of acid centers of medium strength. However, the 5%Cu–1%Pt/BEA sample showed much lower total acidity than the other samples. The 5%Cu–1%Pt/BEA calcined catalyst showed a lower total acidity than the 5%Cu/BEA system. The bimetallic 5%Cu–1%Pt/BEA catalyst exhibited a higher number of moderate-strength acid centers, a similar number of strong-strength acid centers and half the number of weak-strength acid centers compared to the monometallic catalyst. The reduction of copper catalysts and copper–ruthenium (or platinum) catalysts supported on the BEA zeolite resulted in a decrease in total acidity compared to the non-reduced catalysts. The total acidity of the bimetallic reduced catalysts is arranged in descending order: 10%Cu/BEA > 5%Cu/BEA > 5%Cu–1%Ru/BEA > 5%Cu–1%Pt/BEA. The reduction of the 5%Cu/BEA catalyst resulted in a slight increase in the number of acid centers of moderate strength, while maintaining a similar number of acid centers of high strength and a significant reduction in the number of acid centers of weak strength. However, in the case of the 10%Cu/BEA catalyst after reduction, the number of acid centers of moderate strength is comparable to the same catalyst after calcination, while the number of acid centers of weak and high strength on the surface is lower than for the calcined catalyst. Bimetallic catalysts after reduction are characterized by a similar total acidity and the distribution of acid centers of weak, moderate and high strength. The 5%Cu–1%Ru/BEA catalyst sample after reduction is characterized by a much lower number of low-strength acid centers, with a slight decrease in medium- and high-strength acid centers compared to the monometallic catalyst after reduction. The total acidity of the reduced 5%Cu–1%Pt/BEA catalyst is slightly lower than that of the calcined catalyst.

Table 3. The amount of NH₃ desorbed from the support (calcined in an air atmosphere for 4 h at 500 °C), monometallic copper and bimetallic copper–noble metal catalysts after calcination and reduction was calculated from the temperature-programmed desorption (TPD) profiles.

Catalytic Systems	Distribution of Acid Centers			Total Acidity (mmol/g) 100–600 °C
	Weak (mmol/g) 100–300 °C	Moderate (mmol/g) 300–450 °C	Strong (mmol/g) 450–600 °C	
5%Cu/BEA (calc.)	1.54	1.03	0.76	3.33
10%Cu/BEA (calc.)	1.46	1.22	1.17	3.85
5%Cu–1%Ru/BEA (calc.)	1.50	1.15	0.74	3.39
5%Cu–1%Pt/BEA (calc.)	0.78	1.16	0.75	2.69
5%Cu/BEA (red. 300 °C/2 h)	1.02	1.24	0.79	3.05
10%Cu/BEA (red. 300 °C/2 h)	1.15	1.23	0.90	3.28
5%Cu–1%Ru/BEA (red. 400 °C/2 h)	0.84	1.08	0.66	2.58
5%Cu–1%Pt/BEA (red. 300 °C/2 h)	0.76	1.09	0.66	2.51

Desorption peaks visible on the TPD profiles of copper catalysts occurring in the temperature range of 150–200 °C are attributed to the adsorption of ammonia on Lewis centers, i.e., on Al centers, on which the NH₃ bond is weak [50,51]. Desorption peaks located in this temperature range are also attributed to ammonia molecules solvating NH₄⁺ ions (e.g., in N₂H₇⁺ dimers). In the temperature range of 250–450 °C, the desorption peak that occurs corresponds to the more strongly bound ammonia, which is formed from protonated NH₃ produced on the Brønsted acid sites present in the zeolite. The addition of copper causes additional adsorption centers to be produced for ammonia, causing a decrease in the total number of Brønsted acid sites. Ammonia molecules become adsorbed on Cu²⁺ sites [52], which are Lewis acid sites [53]. The strong-strength acid centers present on the surface of copper catalysts deposited on zeolite include places where the desorption temperature is higher than 673 K (400 °C) [54,55]. TPD–NH₃ profiles containing such desorption peaks with maxima at such desorption temperatures are associated with adsorbed NH₃ on Brønsted centers with high acid strength (i.e., Si–O(H)–Al sites) [50,53]. The results of the catalytic activity of the tested monometallic and bimetallic Cu–Ru and Cu–Pt catalysts supported on BEA zeolite showed that higher yields of the obtained methyl esters were obtained for the catalysts after calcination (except for the 5%Cu–1%Pt/BEA catalyst). As mentioned earlier, catalyst reduction reduces total acidity, primarily by reducing the number of weak acid centers. A decrease in FAME efficiency was observed for the catalysts after reduction.

2.5. Phase Composition Studies of Mono and Bimetallic Catalysts

In order to determine the phase composition of monometallic and bimetallic copper catalysts supported on zeolite, XRD analysis was carried out. The XRD results are illustrated in Figure 4. On the XRD pattern of the analyzed 10%Cu/BEA calcined catalyst, there are characteristic diffraction peaks at $2\Theta = 32.6^\circ; 35.5^\circ; 38.7^\circ; 48.8^\circ; 58.3^\circ$ and 61.7° , which are assigned to the copper(II) oxide (CuO) phase. On the other hand, in the diffractogram recorded for the 5%Cu/BEA catalytic system, only one peak originating from copper oxide is distinct for an 2Θ angle value of 38.7° . X-ray diffraction curve of the 5%Cu–1%Ru/BEA catalyst present reflexes which can be assigned to the copper(II) oxide for the following angle values: $2\Theta = 32.7^\circ; 35.5^\circ; 38.7^\circ; 46.3^\circ; 48.8^\circ; 51.2^\circ$ and 53.4° . Meanwhile, the XRD diffraction curve recorded for the 5%Cu–1%Pt/BEA system shows diffraction peaks assigned also to the CuO phase occurring at the $2\Theta = 32.7^\circ; 35.5^\circ; 38.7^\circ; 46.3^\circ; 48.8^\circ; 51.1^\circ; 53.4^\circ; 56.6^\circ; 58.3^\circ$ and 61.7° . Tang et al. [56], in their X-ray diffraction studies of the Cu/SAPO–44 catalyst, identified also CuO phase for the corresponding diffraction peaks located at $2\Theta = 36.9^\circ$ and 38.9° , respectively. The XRD studies performed for the CuO anode during the phase conversion in lithium-ion batteries was done by Feng and co-workers [57] and they also observed in their studies the presence of the diffraction peaks assigned to the CuO phase which were located at an $2\Theta = 35.544^\circ; 38.709^\circ; 48.717^\circ; 58.265^\circ$ and 61.526° . These individual diffraction peaks are indexed to the (11 $\bar{1}$), (111), (20 $\bar{2}$), (202) and (11 $\bar{3}$) crystal planes. The XRD curve of the 5%Cu–1%Ru/BEA catalytic system besides of the diffraction peaks assigned to the CuO phase also exhibits reflexes assigned to ruthenium oxide (RuO₂) phase positioned at an 2Θ angles of $27.9^\circ; 34.9^\circ; 39.9^\circ; 40.4^\circ$ and 54.5° . The similar diffraction peaks located at the 2Θ angles of $28^\circ; 35^\circ$ and 54° and assigned also to RuO₂ phase was observed by Devadas and co-authors in their work [58]. Cruz et al. [59] also observed the same XRD peaks assigned to the same RuO₂ phase during the phase composition studies of RuO₂ electrocatalyst calcined at 350 °C. The same phase of RuO₂ was also detected for the investigated nanoparticles by Sivakami and co-authors [60]. Whereas, on the X-ray diffraction pattern recorded for the studied 5% Cu–1% Pt/BEA catalyst, the faintly visible diffraction peaks positioned at the 2Θ angle of $31.6^\circ; 36.6^\circ$ and 41.0° were identified and assigned to the PtO₂ phase. The remaining diffraction peaks visible in the diffractograms recorded for all catalysts (marked with a corresponding symbol in the Figure 4) are assigned to the zeolite support (BEA).

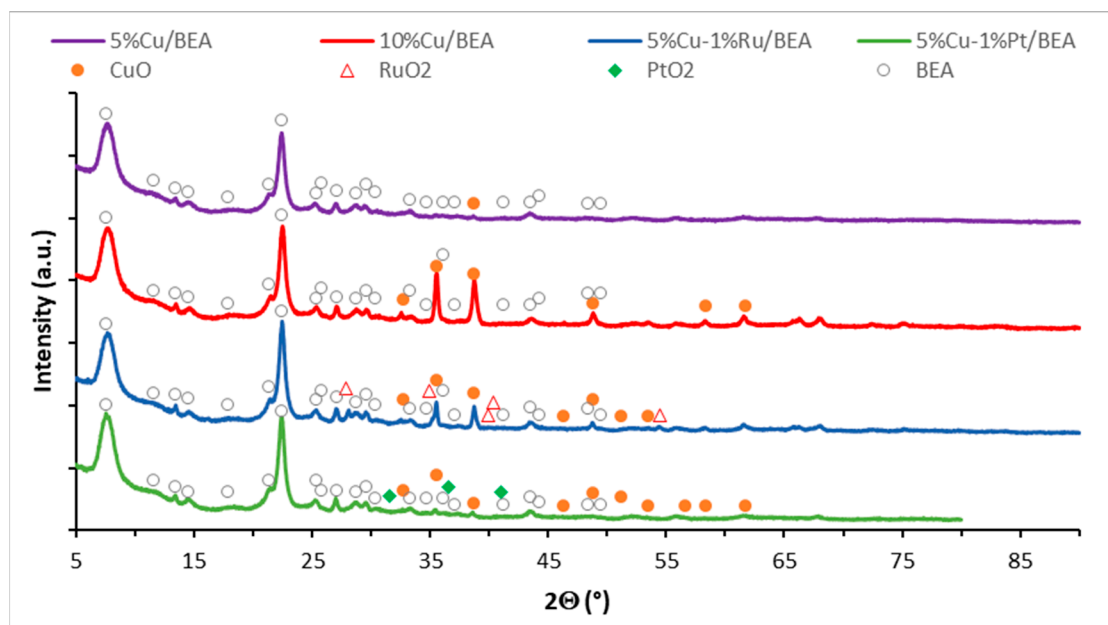


Figure 4. XRD diffraction curves of the calcined 5%Cu/BEA, 10%Cu/BEA, 5%Cu–1%Ru/BEA and 5%Cu–1%Pt/BEA catalysts in an air atmosphere at 500 °C for 4 h.

2.6. Morphology of the Mono and Bimetallic Catalysts

Scanning electron microscopy measurements were carried out for the prepared copper-based zeolite catalysts. This technique allows to determine the morphology and the composition of the catalytic material surface. Figures 5–8 present SEM images that were collected from the surfaces of the calcined systems along with EDS spectra. Figure 5 shows the images and EDS spectrum for the investigated monometallic 5%Cu/BEA catalyst. Elemental composition analysis showed the presence of Cu, O, Si and Al elements on the surface of the studied catalyst. The SEM-EDS measurements performed for this catalyst confirmed a fairly homogeneous distribution of copper on the investigated surface. In the case of the 10%Cu/BEA catalyst the SEM-EDS images, the elemental mapping and EDS spectrum for this system are shown in Figure 6. The EDS elemental maps recorded for the 10%Cu/BEA catalyst show the spatial distribution of elements on the studied micro-area. The EDS elemental mapping obtained for this catalyst clearly shows the presence of copper clusters on the surface. This result showed that the copper dispersion on the surface is not homogeneous. Figure 7 shows SEM-EDS images and the EDS spectrum collected from the surface of the bimetallic 5%Cu–1%Pt/BEA system. Cu, O, Si, Al and Pt were identified on the surface of this catalyst. The EDS elemental mapping performed for this system showed a relatively uniform distribution of copper on the surface, only at some points in the studied micro-area a higher concentration of this element was detected. However, the distribution of platinum in this system is homogeneous.

The last catalyst investigated by SEM-EDS technique (5% Cu–1% Ru/BEA–4) showed the presence of Cu, O, Si, Al, and Ru elements on its surface, consistent with its composition (see Figure 8). However, it should be noted that the distribution of copper and ruthenium is not uniform, as elemental maps show areas with higher concentrations of copper and ruthenium elements. All studied catalysts were prepared by wet impregnation or co-impregnation method, so the presence of areas on the surface with higher concentration of the studied active phase components is logical.

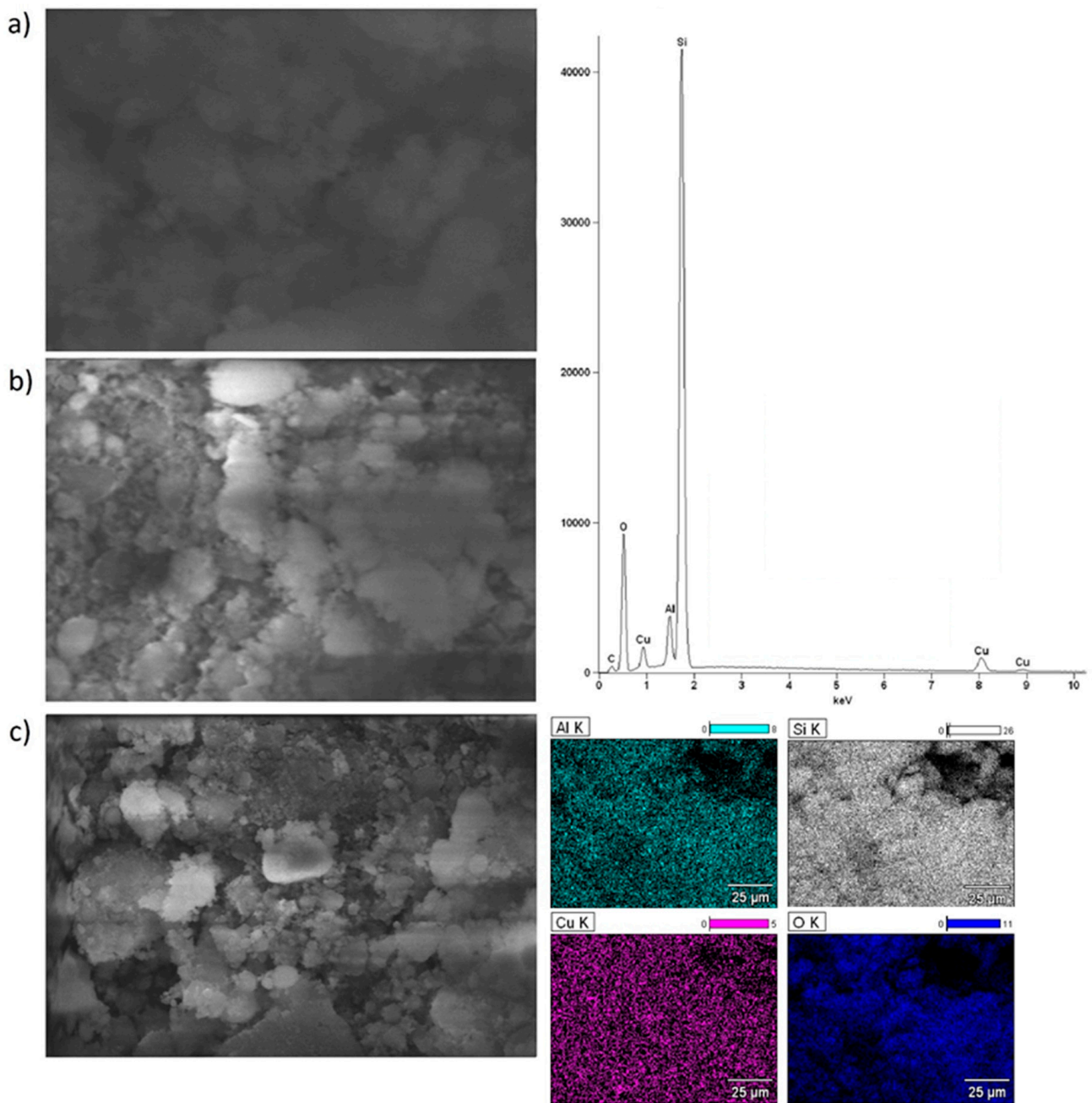


Figure 5. SEM-EDS images (a)—magnification 5000×; (b)—magnification 2500×; and (c)—magnification 1000×; EDS elemental mapping and EDS spectrum recorded for 5%Cu/BEA catalyst after calcination at 500 °C for 4 h in an air atmosphere.

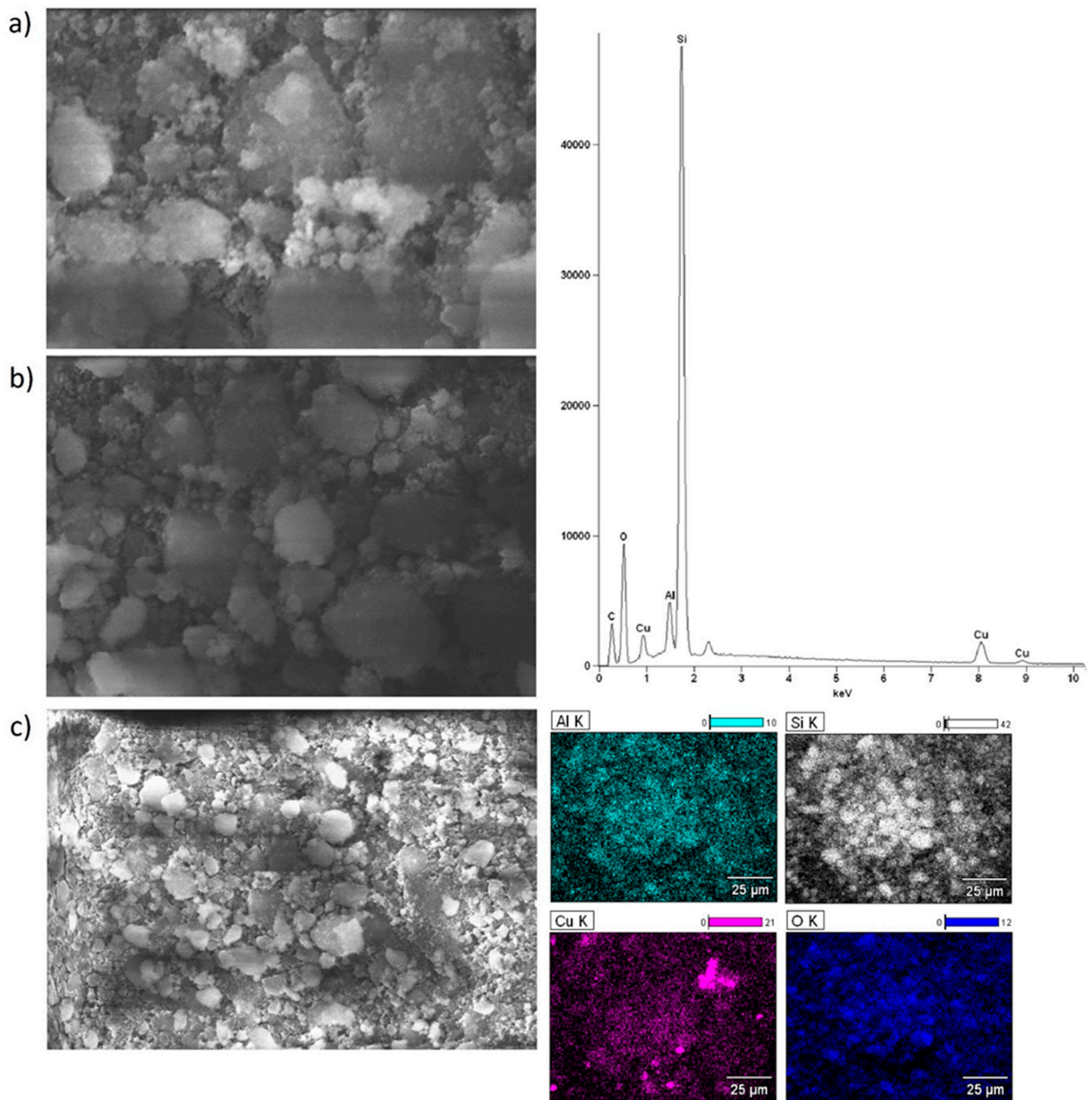


Figure 6. SEM-EDS images (a)—magnification 5000×; (b)—magnification 2500×; (c)—magnification 1000×; EDS elemental mapping and EDS spectrum recorded for 10%Cu/BEA catalyst after calcination at 500 °C for 4 h in an air atmosphere.

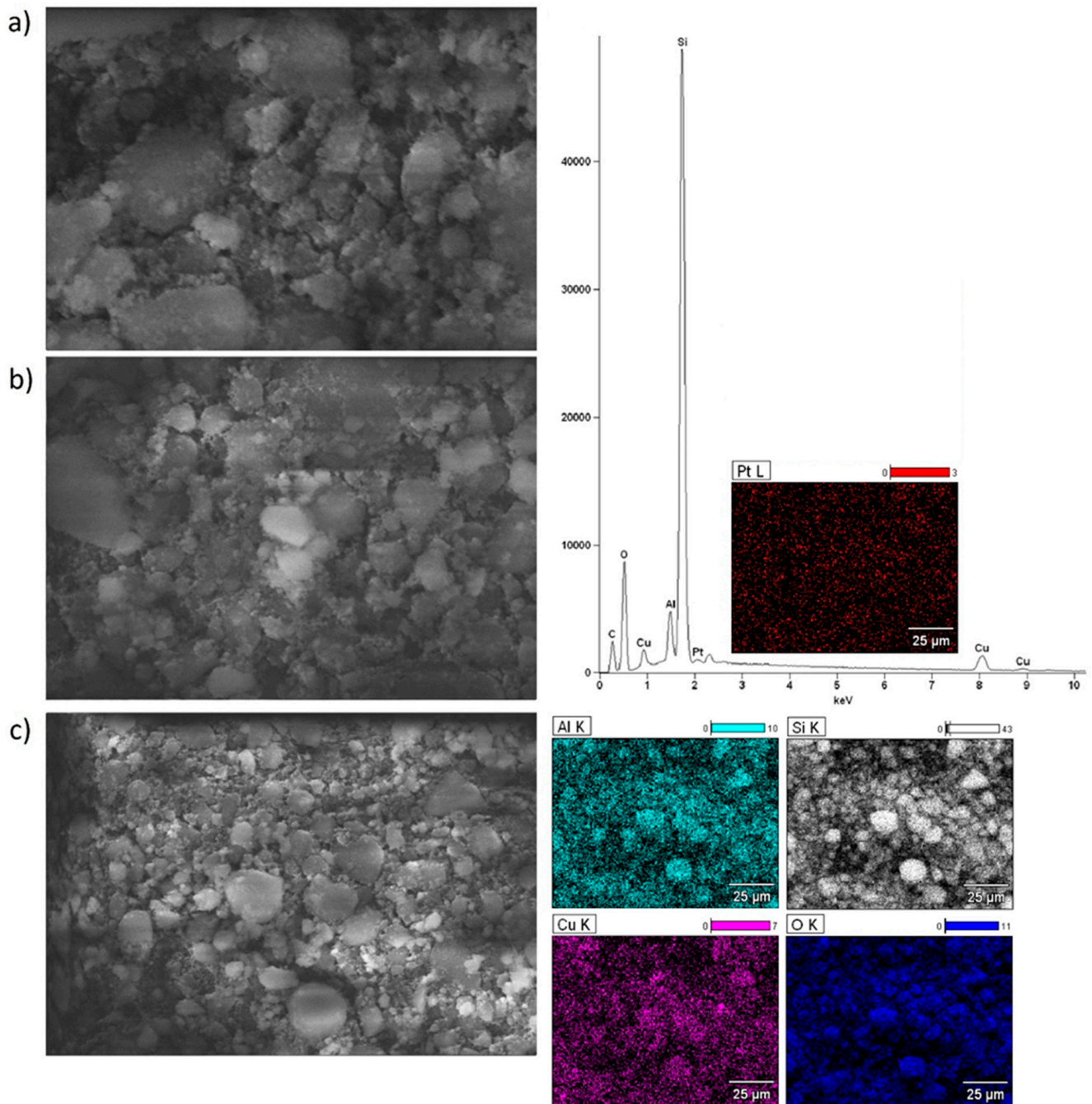


Figure 7. SEM-EDS images (a)—magnification 5000 \times ; (b)—magnification 2500 \times ; (c)—magnification 1000 \times ; EDS elemental mapping and EDS spectrum recorded for 5%Cu–1%Pt/BEA catalyst after calcination at 500 $^{\circ}\text{C}$ for 4 h in an air atmosphere.

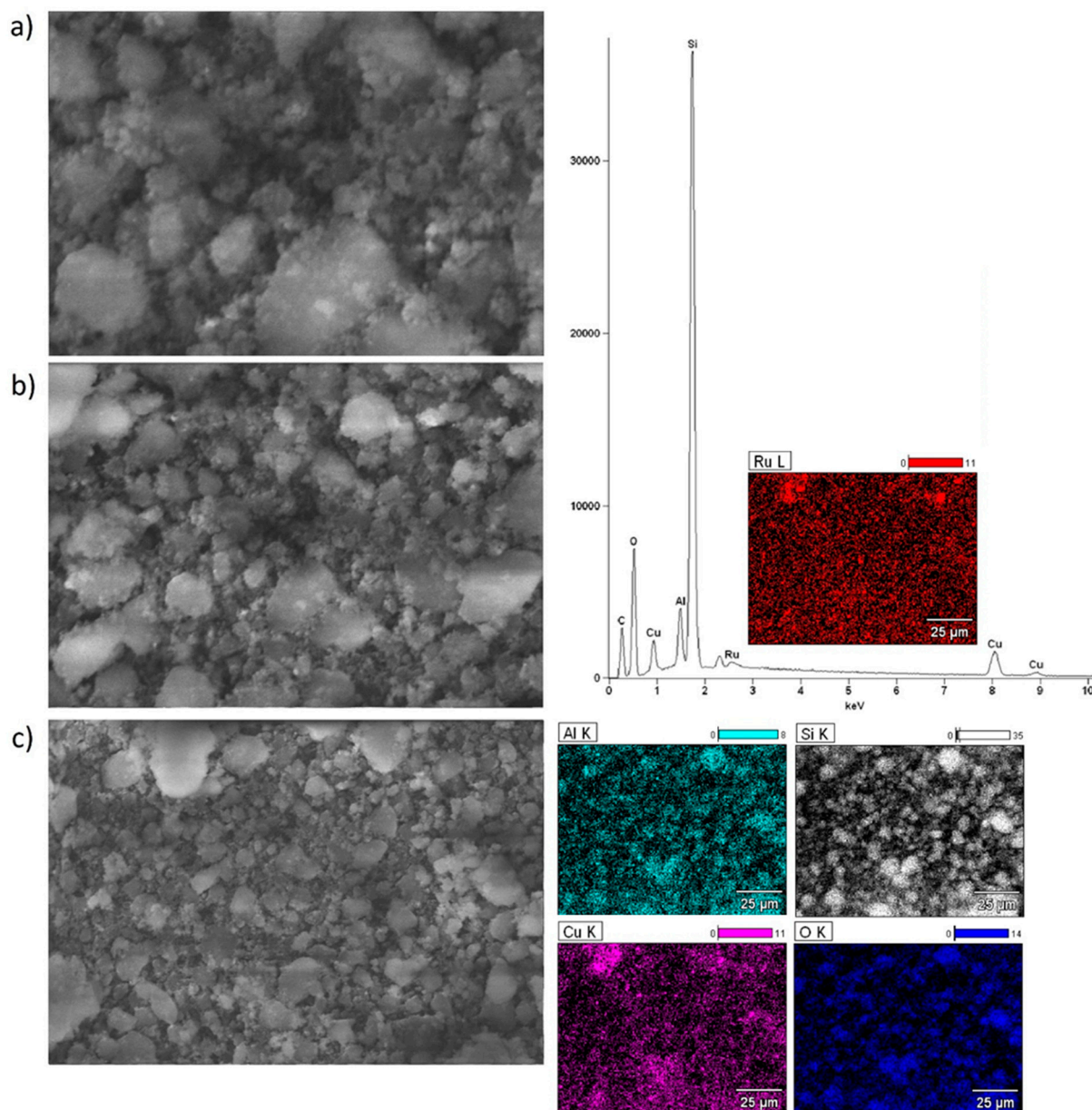


Figure 8. SEM-EDS images (a)—magnification 5000×; (b)—magnification 2500×; (c)—magnification 1000×; EDS elemental mapping and EDS spectrum recorded for 5%Cu–1%Ru/BEA catalyst after calcination at 500 °C for 4 h in an air atmosphere.

3. Materials and Methods

3.1. Materials

An ammonium form of zeolite BEA (NH₄-BEA) with a silicon to aluminum ratio of 25 was purchased from Zeolyst International (Kansas City, KS, USA). Copper nitrate trihydrate (Cu(NO₃)₂·3H₂O)(CHEMPUR, purity 99.0%) was used as a precursor of the active phase of the copper based catalysts. Hexachloroplatinic acid (Sigma Aldrich, Poznan, Poland) and ruthenium chloride (Sigma Aldrich) were used as suitable precursors of noble metals during the preparation of bimetallic catalysts.

3.2. Preparation of Mono- and Bimetallic Cu–Zeolite Catalysts

Cu/BEA catalysts were synthesized by a wet impregnation method using the hydrogen form of BEA zeolite. The hydrogen form of zeolite BEA was obtained by converting the ammonium form of zeolite NH₄-BEA by calcination of support in a muffle furnace for

20 h at 500 °C in an air atmosphere. Then, the zeolite support was impregnated for 24 h. The copper content of the zeolite catalysts was 5 wt.% and 10 wt.%, respectively. Bimetallic Cu–noble metal catalysts were synthesized by co-impregnation method. According to this method, an appropriate amount of copper (5 wt.%) and noble metal platinum or ruthenium (1 wt.%) were added to the support. After impregnation, the catalysts were dried at 120 °C for 2 h. The resulting solid was calcined in a muffle furnace at 500 °C for 4 h in an air atmosphere.

3.3. Catalyst Characterization

The phase composition of the synthesized catalytic materials was determined using the X-ray diffraction technique in a PANalytical X'Pert Pro MPD diffractometer (Malvern Panalytical Ltd., Royston, UK) in Bragg–Brentano reflection geometry. Cu K_{α} radiation ($k = 154.05$ pm) from a sealed tube was used in the 2θ angle range 5–90°. The catalyst surface morphology was investigated using an S-4700 scanning electron microscope HITACHI (Tokyo, Japan), equipped with an energy dispersive spectrometer (ThermoNoran, Madison, WI, USA) (SEM–EDS). The reducibility of the monometallic copper–zeolite and bimetallic catalysts supported on ZSM-5 zeolite was investigated via the temperature-programmed reduction technique (TPR- H_2), using an automatic AMI-1 instrument (Altamira Instruments, Pittsburgh, PA, USA). The reduction behaviour of the catalytic materials was determined in the temperature range of 35–900 °C. The consumption of hydrogen was monitored by a thermal conductivity detector (TCD). The temperature-programmed desorption of ammonia technique (TPD- NH_3) was used to determine the acidity of the investigated catalytic systems. TPD- NH_3 measurements were performed in a quartz microreactor. Ammonia was used as a probe molecule. The adsorption of ammonia occurred on the catalyst surface at a temperature of 100 °C for 15 min after purification of the tested sample in a helium stream (40 mL/min) at a temperature of 500 °C for 60 min. After NH_3 adsorption, the system was purged with helium stream at a flow rate of 40 mL/min to remove physically adsorbed ammonia. TPD- NH_3 measurements were carried out in the temperature range of 100–600 °C at a helium flow rate (40 mL/min), and the desorption of ammonia gas from the acidic sites of the catalyst was identified using a TCD detector. Before the experiment, catalyst samples were reduced “in situ” at 300 °C (or by 400 °C) for 2 h in a reducing mixture (5% H_2 –95%Ar). The specific surface area of the prepared catalysts was determined by low temperature nitrogen adsorption–desorption measurements were carried out using BET, liquid N_2 method. During the measurements a Micrometrics ASAP 2020 analyser was used. The Brunauer–Emmett–Teller (BET) method was used to determine the total surface area and pore volume, while the micropore volumes and micropore surface area were determined using the t-plot method. The average pore size was determined using the Barrett–Joyner–Halenda (BJH) model.

3.4. Reaction Conditions

The transesterification reaction was carried out in an autoclave (manufactured by Parr USA, reactor volume 50 mL) equipped with a mechanical stirrer. Transesterification reactions were carried out at 220 °C for 2 h. The reaction mixture consisted of oil and methanol in a molar ratio of 9:1 (methanol/oil). The methanol used in this reaction was purchased from CHEMPUR, Poland. Before the reaction tests, the monometallic and bimetallic copper catalysts were calcined in an air atmosphere at 500 °C for 4 h. In order to determine the influence of the reduction process on the catalytic properties of the synthesized catalysts in transesterification reaction, second series of the catalytic materials were prepared. The second series of the catalysts were also calcined at the same conditions as before mentioning catalysts and reduced in a mixture of 5% H_2 –95Ar at 300 or 400 °C depending on the catalyst. All copper supported catalysts were reduced at 300 °C for 2 h in a mixture of 5% H_2 –95% Ar. The reduction process of the copper–platinum catalyst was performed at 300 °C for 2 h in a mixture of 5% H_2 –95% Ar. While, copper–ruthenium catalysts were reduced in the same reduction mixture at 400 °C for two hours. The flow

rate of the reducing mixture was 50 cm³/min. In all reactivity tests the catalyst loading was 0.5 g.

3.5. Analysis of Transesterification Products and Determination of TG Conversion

The reaction products obtained as a result of the transesterification reaction were analyzed using the HPLC technique (Shimadzu). All analyses used column C-18 (5 μm, 4.6 × 250) and a mixture of 2-isopropanol-hexane (4/5) and methanol as eluent. All chemicals were purchased from CHEMPUR, Poland. The mobile phase gradient applied in each experiment is shown in Table 4. The reaction products were analyzed with a DAD detector (wavelength: λ = 205 nm) to define triglyceride conversion and FAME yield. TG conversion was calculated according to the equation based also on HPLC analysis.

$$\text{Conv. (\%)} = \frac{TG_{in} - TG_{out}}{TG_{in}} \times 100\%$$

where: TG_{in} —the total area under the peaks assigned to the TG in rapeseed oil, and TG_{out} —the sum of the areas of TG peaks in the product.

Table 4. Phase gradient used in the HPLC measurements.

Time [min]	Mobile Phase Gradient		Flow Rate [mL/min]
	Solvent A (%)	Solvent B (%)	
0	100	0	0.9
20	100	0	0.9
45	0	100	0.9
70	0	100	0.9
75	100	0	0.9

Solvent A: Methanol; Solvent B: 2-Propanol/Hexane = 4/5; Injection Volume: 25 μL; Column Temperature: 25 °C.

4. Conclusions

This work presents the catalytic and physicochemical properties of copper catalysts and copper–noble metal (ruthenium, platinum) catalysts on BEA zeolite prepared using impregnation (monometallic systems) and co-impregnation methods. The physicochemical properties of the studied catalytic systems were investigated using TPR-H₂, XRD, TPD-NH₃ and SEM-EDS techniques, and their correlation with catalytic activity in biodiesel production via the transesterification reaction of vegetable oil with methanol was established. The results of the catalytic activity obtained in the transesterification reaction for calcined and reduced catalysts indicate the possibility of their application in the investigated process. Higher TG conversion and FAME yields were observed for all systems that were not reduced. Calcined catalysts showed higher total acidity in TPD-NH₃ tests compared to the reduced counterparts. Lower acidity was observed in the case of reduced catalysts, mainly due to a decrease in the number of weak-strength acid centers. This is reflected in the FAME yields, which were higher in the reaction conducted over non-reduced catalysts. Increasing the amount of copper from 5 wt.% to 10 wt.% in a monometallic catalyst improved FAME yields by about 10%, while introducing ruthenium or platinum at 1 wt.% improved TG conversion by about 10% with a slight improvement in FAME yield, in comparison to a monometallic catalyst. The surface morphology investigations performed using the SEM-EDS technique showed that the monometallic catalysts with higher copper content (10% Cu/BEA) and the bimetallic catalyst (5% Cu–1% Ru/BEA) owned areas on their surface with increased concentration of the active phase components, while in the other catalysts the distribution of the active phase components on the surface was relatively uniform. The highest biodiesel yield (61.6%) was obtained in the reaction performed over non-reduced 10%Cu/BEA catalyst at a high oil conversion of 75.7%. In contrast, the highest triglyceride conversion (85.1%) was observed for the transesterification reaction realized on the calcined

5%Cu–1%Ru/BEA system. The FAME yield for this system was 58.4% and this was the second highest among all the tested catalytic materials.

Author Contributions: Conceptualization, M.I.S.-J. and P.M.; Methodology, P.M.; Software, Ł.S.; Validation, Ł.S. and P.M.; Formal analysis, P.M.; Investigation, Ł.S., W.M. and J.A.; Resources, P.M.; Data curation, Ł.S.; Writing—original draft, Ł.S. and P.M.; Writing—review & editing, P.M.; Visualization, Ł.S.; Supervision, K.C.-Ś., M.I.S.-J. and P.M.; Project administration, P.M. All authors have read and agreed to the published version of the manuscript.

Funding: This research received no external funding.

Data Availability Statement: Data are contained within the article.

Acknowledgments: This article has been completed while the first author was the Doctoral Candidate in the Interdisciplinary Doctoral School at the Lodz University of Technology, Poland.

Conflicts of Interest: The authors declare no conflict of interest.

References

1. Gardy, J.; Nourafkan, E.; Osatiashiani, A.; Lee, A.F.; Wilson, K.; Hassanpour, A.; Lai, X. A core-shell $\text{SO}_4/\text{Mg-Al-Fe}_3\text{O}_4$ catalyst for biodiesel production. *Appl. Catal. B Environ.* **2019**, *259*, 118093. [CrossRef]
2. Behera, B.; Selvam, S.M.; Dey, B.; Balasubramanian, P. Algal biodiesel production with engineered biochar as a heterogeneous solid acid catalyst. *Bioresour. Technol.* **2020**, *310*, 123392. [CrossRef] [PubMed]
3. Khatibi, M.; Khorasheh, F.; Larimi, A. Biodiesel production via transesterification of canola oil in the presence of Na-K doped CaO derived from calcined eggshell. *Renew. Energy* **2021**, *163*, 1626–1636. [CrossRef]
4. Alvarez Serafini, M.S.; Tonetto, G.M. Synthesis of Fatty Acid Methyl Esters from Pomace Oil Catalyzed by Zinc Stearate: A Kinetic Study of the Transesterification and Esterification Reactions. *Catalysts* **2019**, *9*, 978. [CrossRef]
5. Chen, C.-L.; Huang, C.-C.; Ho, K.-C.; Hsiao, P.-X.; Wu, M.-S.; Chang, J.-S. Biodiesel production from wet microalgae feedstock using sequential wet extraction/transesterification and direct transesterification processes. *Bioresour. Technol.* **2015**, *194*, 179–186. [CrossRef] [PubMed]
6. Vasić, K.; Hojnik Podrepšek, G.; Knez, Ž.; Leitgeb, M. Biodiesel Production Using Solid Acid Catalysts Based on Metal Oxides. *Catalysts* **2020**, *10*, 237. [CrossRef]
7. Xu, C.; Enache, D.I.; Lloyd, R.; Knight, D.W.; Bartley, J.K.; Hutchings, G.J. Mgo Catalysed Triglyceride Transesterification for Biodiesel Synthesis. *Catal. Lett.* **2010**, *138*, 1–7. [CrossRef]
8. Szkudlarek, Ł.; Chałupka, K.; Maniukiewicz, W.; Albińska, J.; Szykowska-Jóźwik, M.I.; Mierczyński, P. The influence of si/al ratio on the physicochemical and catalytic properties of mgo/zsm-5 catalyst in transesterification reaction of rapeseed oil. *Catalysts* **2021**, *11*, 1260. [CrossRef]
9. Szkudlarek, Ł.; Chałupka-Śpiewak, K.; Maniukiewicz, W.; Nowosielska, M.; Szykowska-Jóźwik, M.I.; Mierczyński, P. Biodiesel Production by Methanolysis of Rapeseed Oil—Influence of $\text{SiO}_2/\text{Al}_2\text{O}_3$ Ratio in BEA Zeolite Structure on Physicochemical and Catalytic Properties of Zeolite Systems with Alkaline Earth Oxides (MgO, CaO, SrO). *Int. J. Mol. Sci.* **2024**, *25*, 3570. [CrossRef]
10. Mierczynski, P.; Szkudlarek, Ł.; Chalupka, K.; Maniukiewicz, W.; Wahono, S.K.; Vasilev, K.; Szykowska-Jozwik, M.I. The Effect of the Activation Process and Metal Oxide Addition (CaO, MgO, SrO) on the Catalytic and Physicochemical Properties of Natural Zeolite in Transesterification Reaction. *Materials* **2021**, *14*, 2415. [CrossRef]
11. Mierczynski, P.; Mosińska, M.; Szkudlarek, Ł.; Chalupka, K.; Tatsuzawa, M.; Al Maskari, M.; Maniukiewicz, W.; Wahono, S.K.; Vasilev, K.; Szykowska-Jozwik, M.I. Biodiesel Production on Monometallic Pt, Pd, Ru, and Ag Catalysts Supported on Natural Zeolite. *Materials* **2021**, *14*, 48. [CrossRef] [PubMed]
12. Xie, W.; Han, Y.; Wang, H. Magnetic $\text{Fe}_3\text{O}_4/\text{MCM-41}$ composite-supported sodium silicate as heterogeneous catalysts for biodiesel production. *Renew. Energy* **2018**, *125*, 675–681. [CrossRef]
13. Xie, W.; Gao, C.; Li, J. Sustainable biodiesel production from low-quantity oils utilizing $\text{H}_6\text{PV}_3\text{MoW}_8\text{O}_{40}$ supported on magnetic $\text{Fe}_3\text{O}_4/\text{ZIF-8}$ composites. *Renew. Energy* **2021**, *168*, 927–937. [CrossRef]
14. Xie, W.; Li, J. Magnetic solid catalysts for sustainable and cleaner biodiesel production: A comprehensive review. *Renew. Sustain. Energy Rev.* **2023**, *171*, 113017. [CrossRef]
15. Sulaiman, N.F.; Ramly, N.I.; Abd Mubin, M.H.; Lee, S.L. Transition metal oxide (NiO, CuO, ZnO)-doped calcium oxide catalysts derived from eggshells for the transesterification of refined waste cooking oil. *RSC Adv.* **2021**, *11*, 21781–21795. [CrossRef] [PubMed]
16. Liu, X.; He, H.; Wang, Y.; Zhu, S. Transesterification of soybean oil to biodiesel using SrO as a solid base catalyst. *Catal. Commun.* **2007**, *8*, 1107–1111. [CrossRef]
17. Zhang, C.-Y.; Shao, W.-L.; Zhou, W.-X.; Liu, Y.; Han, Y.-Y.; Zheng, Y.; Liu, Y.-J. Biodiesel Production by Esterification Reaction on K+ Modified MgAl-Hydrotalcites Catalysts. *Catalysts* **2019**, *9*, 742. [CrossRef]

18. Machorro, J.J.; Lazaro, A.L.; Espejel-Ayala, F.; Coutiño-Gonzalez, E.; Chavarria-Hernandez, J.C.; Godínez, L.A.; Rodríguez-Valadez, F.J. The Roles of the Structure and Basic Sites of Sodium Titanates on Transesterification Reactions to Obtain Biodiesel. *Catalysts* **2019**, *9*, 989. [\[CrossRef\]](#)
19. Enguilo Gonzaga, V.; Romero, R.; Gómez-Espinosa, R.M.; Romero, A.; Martínez, S.L.; Natividad, R. Biodiesel Production from Waste Cooking Oil Catalyzed by a Bifunctional Catalyst. *ACS Omega* **2021**, *6*, 24092–24105. [\[CrossRef\]](#)
20. Al-Muhtaseb, A.a.H. Utilisation of Non-Edible Source (*Pongamia pinnata* Seeds Shells) for Producing Methyl Esters as Cleaner Fuel in the Presence of a Novel Heterogeneous Catalyst Synthesized from Waste Eggshells. *Molecules* **2021**, *26*, 5772. [\[CrossRef\]](#)
21. Pang, H.; Yang, G.; Li, L.; Yu, J. Efficient transesterification over two-dimensional zeolites for sustainable biodiesel production. *Green Energy Environ.* **2020**, *5*, 405–413. [\[CrossRef\]](#)
22. Lani, N.S.; Ngadi, N.; Inuwa, I.M.; Opotu, L.A.; Zakaria, Z.Y.; Widayat, W. Influence of desilication route of ZSM-5 zeolite in mesoporous zeolite supported calcium oxide catalyst for biodiesel production. *Microporous Mesoporous Mater.* **2022**, *343*, 112153. [\[CrossRef\]](#)
23. Orlyk, S.; Kyriienko, P.; Kapran, A.; Chedryk, V.; Balakin, D.; Gurgul, J.; Zimowska, M.; Millot, Y.; Dzwigaj, S. CO₂-Assisted Dehydrogenation of Propane to Propene over Zn-BEA Zeolites: Impact of Acid–Base Characteristics on Catalytic Performance. *Catalysts* **2023**, *13*, 681. [\[CrossRef\]](#)
24. Lee, K.; Kosaka, H.; Sato, S.; Yokoi, T.; Choi, B.; Kim, D. Effects of Cu loading and zeolite topology on the selective catalytic reduction with C₃H₆ over Cu/zeolite catalysts. *J. Ind. Eng. Chem.* **2019**, *72*, 73–86. [\[CrossRef\]](#)
25. Pereda-Ayo, B.; De La Torre, U.; Illán-Gómez, M.J.; Bueno-López, A.; González-Velasco, J.R. Role of the different copper species on the activity of Cu/zeolite catalysts for SCR of NO_x with NH₃. *Appl. Catal. B Environ.* **2014**, *147*, 420–428. [\[CrossRef\]](#)
26. Witsuthammakul, A.; Sooknoi, T. Selective hydrodeoxygenation of bio-oil derived products: Acetic acid to propylene over hybrid CeO₂-Cu/zeolite catalysts. *Catal. Sci. Technol.* **2016**, *6*, 1737–1745. [\[CrossRef\]](#)
27. Xing, X.; Li, N.; Sun, Y.; Wang, G.; Cheng, J.; Hao, Z. Selective catalytic oxidation of n-butylamine over Cu-zeolite catalysts. *Catal. Today* **2020**, *339*, 192–199. [\[CrossRef\]](#)
28. Moreno-González, M.; Blasco, T.; Góra-Marek, K.; Palomares, A.E.; Corma, A. Study of propane oxidation on Cu-zeolite catalysts by in-situ EPR and IR spectroscopies. *Catal. Today* **2014**, *227*, 123–129. [\[CrossRef\]](#)
29. Kumar, R.; Strezov, V.; Lovell, E.; Kan, T.; Weldekidan, H.; He, J.; Jahan, S.; Dastjerdi, B.; Scott, J. Enhanced bio-oil deoxygenation activity by Cu/zeolite and Ni/zeolite catalysts in combined in-situ and ex-situ biomass pyrolysis. *J. Anal. Appl. Pyrolysis* **2019**, *140*, 148–160. [\[CrossRef\]](#)
30. Zhu, J.; Sushkevich, V.L.; Knorpp, A.J.; Newton, M.A.; Mizuno, S.C.M.; Wakihara, T.; Okubo, T.; Liu, Z.; van Bokhoven, J.A. Cu-Erionite Zeolite Achieves High Yield in Direct Oxidation of Methane to Methanol by Isothermal Chemical Looping. *Chem. Mater.* **2020**, *32*, 1448–1453. [\[CrossRef\]](#)
31. Brezicki, G.; Zheng, J.; Paolucci, C.; Schlögl, R.; Davis, R.J. Effect of the Co-cation on Cu Speciation in Cu-Exchanged Mordenite and ZSM-5 Catalysts for the Oxidation of Methane to Methanol. *ACS Catal.* **2021**, *11*, 4973–4987. [\[CrossRef\]](#)
32. Zhou, C.; Li, S.; He, S.; Zhao, Z.; Jiao, Y.; Zhang, H. Temperature-dependant active sites for methane continuous conversion to methanol over Cu-zeolite catalysts using water as the oxidant. *Fuel* **2022**, *329*, 125483. [\[CrossRef\]](#)
33. Chang, F.; Yan, C.; Zhou, Q. Synthesis of a New Copper-Based Supramolecular Catalyst and Its Catalytic Performance for Biodiesel Production. *Int. J. Chem. Eng.* **2018**, *2018*, 7452817. [\[CrossRef\]](#)
34. Pangestu, T.; Kurniawan, Y.; Soetaredjo, F.E.; Santoso, S.P.; Irawaty, W.; Yuliana, M.; Hartono, S.B.; Ismadji, S. The synthesis of biodiesel using copper based metal-organic framework as a catalyst. *J. Environ. Chem. Eng.* **2019**, *7*, 103277. [\[CrossRef\]](#)
35. da Silva, R.B.; Lima Neto, A.F.; Soares dos Santos, L.S.; de Oliveira Lima, J.R.; Chaves, M.H.; dos Santos, J.R.; de Lima, G.M.; de Moura, E.M.; de Moura, C.V.R. Catalysts of Cu(II) and Co(II) ions adsorbed in chitosan used in transesterification of soy bean and babassu oils—A new route for biodiesel syntheses. *Bioresour. Technol.* **2008**, *99*, 6793–6798. [\[CrossRef\]](#)
36. Chen, L.; Yin, P.; Liu, X.; Yang, L.; Yu, Z.; Guo, X.; Xin, X. Biodiesel production over copper vanadium phosphate. *Energy* **2011**, *36*, 175–180. [\[CrossRef\]](#)
37. Mierczynski, P.; Ciesielski, R.; Kedziora, A.; Zaborowski, M.; Maniukiewicz, W.; Nowosielska, M.; Szyrkowska, M.I.; Maniecki, T.P. Novel Pd-Cu/ZnAl₂O₄-ZrO₂ Catalysts for Methanol Synthesis. *Catal. Lett.* **2014**, *144*, 723–735. [\[CrossRef\]](#)
38. Mierczynski, P.; Maniecki, T.; Maniukiewicz, W.; Jozwiak, W. Cu/Cr₂O₃ center dot 3Al₂O₃ and Au-Cu/Cr₂O₃ center dot 3Al₂O₃ catalysts for methanol synthesis and water gas shift reactions. *React. Kinet. Mech. Catal.* **2011**, *104*, 139–148. [\[CrossRef\]](#)
39. Schaidle, J.A.; Ruddy, D.A.; Habas, S.E.; Pan, M.; Zhang, G.; Miller, J.T.; Hensley, J.E. Conversion of Dimethyl Ether to 2,2,3-Trimethylbutane over a Cu/BEA Catalyst: Role of Cu Sites in Hydrogen Incorporation. *ACS Catal.* **2015**, *5*, 1794–1803. [\[CrossRef\]](#)
40. Lin, Q.; Liu, J.; Liu, S.; Xu, S.; Lin, C.; Feng, X.; Wang, Y.; Xu, H.; Chen, Y. Barium-promoted hydrothermal stability of monolithic Cu/BEA catalyst for NH₃-SCR. *Dalton Trans.* **2018**, *47*, 15038–15048. [\[CrossRef\]](#)
41. Wang, H.; Xu, R.; Jin, Y.; Zhang, R. Zeolite structure effects on Cu active center, SCR performance and stability of Cu-zeolite catalysts. *Catal. Today* **2019**, *327*, 295–307. [\[CrossRef\]](#)
42. Mierczynski, P.; Maniecki, T.P.; Chalupka, K.; Maniukiewicz, W.; Jozwiak, W.K. Cu/Zn_xAl_yO_z supported catalysts (ZnO: Al₂O₃ = 1, 2, 4) for methanol synthesis. *Catal. Today* **2011**, *176*, 21–27. [\[CrossRef\]](#)
43. Mierczynski, P.; Vasilev, K.; Mierczynska, A.; Maniukiewicz, W.; Maniecki, T.P. Highly selective Pd-Cu/ZnAl₂O₄ catalyst for hydrogen production. *Appl. Catal. A Gen.* **2014**, *479*, 26–34. [\[CrossRef\]](#)

44. Mierczynski, P.; Maniukiewicz, W.; Maniecki, T.P. Comparative studies of Pd, Ru, Ni, Cu/ZnAl₂O₄ catalysts for the water gas shift reaction. *Cent. Eur. J. Chem.* **2013**, *11*, 912–919. [[CrossRef](#)]
45. Nurunnabi, M.; Murata, K.; Okabe, K.; Inaba, M.; Takahara, I. Effect of Mn addition on activity and resistance to catalyst deactivation for Fischer–Tropsch synthesis over Ru/Al₂O₃ and Ru/SiO₂ catalysts. *Catal. Commun.* **2007**, *8*, 1531–1537. [[CrossRef](#)]
46. Serrano, D.P.; Escola, J.M.; Briones, L.; Medina, S.; Martínez, A. Hydroreforming of the oils from LDPE thermal cracking over Ni–Ru and Ru supported over hierarchical Beta zeolite. *Fuel* **2015**, *144*, 287–294. [[CrossRef](#)]
47. Glotov, A.; Vutolkina, A.; Pimerzin, A.; Nedolivko, V.; Zasyalov, G.; Stytsenko, V.; Karakhanov, E.; Vinokurov, V. Ruthenium Catalysts Templated on Mesoporous MCM-41 Type Silica and Natural Clay Nanotubes for Hydrogenation of Benzene to Cyclohexane. *Catalysts* **2020**, *10*, 537. [[CrossRef](#)]
48. Pérez-Bustos, H.F.; Lucio-Ortiz, C.J.; de la Rosa, J.R.; de Haro del Río, D.A.; Sandoval-Rangel, L.; Martínez-Vargas, D.X.; Maldonado, C.S.; Rodríguez-González, V.; Garza-Navarro, M.A.; Morales-Leal, F.J. Synthesis and characterization of bimetallic catalysts Pd–Ru and Pt–Ru supported on γ -alumina and zeolite FAU for the catalytic transformation of HMF. *Fuel* **2019**, *239*, 191–201. [[CrossRef](#)]
49. Xie, J.; Sun, X.; Barrett, L.; Walker, B.R.; Karote, D.R.; Langemeier, J.M.; Leaym, X.; Kroh, F.; Traylor, W.; Feng, J.; et al. Autothermal reforming and partial oxidation of n-hexadecane via Pt/Ni bimetallic catalysts on ceria-based supports. *Int. J. Hydrogen Energy* **2015**, *40*, 8510–8521. [[CrossRef](#)]
50. Gao, F.; Washton, N.M.; Wang, Y.; Kollár, M.; Szanyi, J.; Peden, C.H.F. Effects of Si/Al ratio on Cu/SSZ-13 NH₃-SCR catalysts: Implications for the active Cu species and the roles of Brønsted acidity. *J. Catal.* **2015**, *331*, 25–38. [[CrossRef](#)]
51. Beale, A.M.; Gao, F.; Lezcano-Gonzalez, I.; Peden, C.H.F.; Szanyi, J. Recent advances in automotive catalysis for NO_x emission control by small-pore microporous materials. *Chem. Soc. Rev.* **2015**, *44*, 7371–7405. [[CrossRef](#)] [[PubMed](#)]
52. Lezcano-Gonzalez, I.; Deka, U.; Arstad, B.; Van Yperen-De Deyne, A.; Hemelsoet, K.; Waroquier, M.; Van Speybroeck, V.; Weckhuysen, B.M.; Beale, A.M. Determining the storage, availability and reactivity of NH₃ within Cu-Chabazite-based Ammonia Selective Catalytic Reduction systems. *Phys. Chem. Chem. Phys.* **2014**, *16*, 1639–1650. [[CrossRef](#)] [[PubMed](#)]
53. Qiu, Y.; Fan, C.; Sun, C.; Zhu, H.; Yi, W.; Chen, J.; Guo, L.; Niu, X.; Chen, J.; Peng, Y.; et al. New Insight into the In Situ SO₂ Poisoning Mechanism over Cu-SSZ-13 for the Selective Catalytic Reduction of NO_x with NH₃. *Catalysts* **2020**, *10*, 1391. [[CrossRef](#)]
54. Ribeiro, N.F.P.; Henriques, C.A.; Schmal, M. Copper-based Catalysts for Synthesis of Methylamines: The Effect of the Metal and the Role of the Support. *Catal. Lett.* **2005**, *104*, 111–119. [[CrossRef](#)]
55. Shutkina, O.V.; Ponomareva, O.A.; Ivanova, I.I. Catalytic synthesis of cumene from benzene and acetone. *Pet. Chem.* **2013**, *53*, 20–26. [[CrossRef](#)]
56. Tang, J.; Xu, M.; Yu, T.; Ma, H.; Shen, M.; Wang, J. Catalytic deactivation mechanism research over Cu/SAPO-34 catalysts for NH₃-SCR (II): The impact of copper loading. *Chem. Eng. Sci.* **2017**, *168*, 414–422. [[CrossRef](#)]
57. Feng, L.; Wang, R.; Zhang, Y.; Ji, S.; Chuan, Y.; Zhang, W.; Liu, B.; Yuan, C.; Du, C. In situ XRD observation of CuO anode phase conversion in lithium-ion batteries. *J. Mater. Sci.* **2019**, *54*, 1520–1528. [[CrossRef](#)]
58. Devadas, A.; Baranton, S.; Napporn, T.W.; Coutanceau, C. Tailoring of RuO₂ nanoparticles by microwave assisted “Instant method” for energy storage applications. *J. Power Sour.* **2011**, *196*, 4044–4053. [[CrossRef](#)]
59. Cruz, J.C.; Baglio, V.; Siracusano, S.; Antonucci, V.; Aricò, A.S.; Ornelas, R.; Ortiz-Frade, L.; Osorio-Monreal, G.; Durón-Torres, S.M.; Arriaga, L.G. Preparation and characterization of RuO₂ catalysts for oxygen evolution in a solid polymer electrolyte. *Int. J. Electrochem. Sci.* **2011**, *6*, 6607–6619. [[CrossRef](#)]
60. Sivakami, R.; Dhanuskodi, S.; Karvembu, R. Estimation of lattice strain in nanocrystalline RuO₂ by Williamson–Hall and size–strain plot methods. *Spectrochim. Acta Part A Mol. Biomol. Spectrosc.* **2016**, *152*, 43–50. [[CrossRef](#)]

Disclaimer/Publisher’s Note: The statements, opinions and data contained in all publications are solely those of the individual author(s) and contributor(s) and not of MDPI and/or the editor(s). MDPI and/or the editor(s) disclaim responsibility for any injury to people or property resulting from any ideas, methods, instructions or products referred to in the content.